

Supporting Information

Highly Emissive Surface Layer in Mixed-Halide Multi-Cation Perovskites

Zahra Andaji-Garmaroudi¹, Mojtaba Abdi-Jalebi¹, Dengyang Guo², Stuart Macpherson¹, Aditya Sadhanala^{1,3}, Elizabeth M. Tennyson¹, Edoardo Ruggeri¹, Miguel Anaya¹, Krzysztof Galkowski^{1,4}, Ravichandran Shivanna¹, Kilian Lohmann¹, Kyle Frohma¹, Sebastian Mackowski⁴, Tom J Savenije², Richard H Friend¹, Samuel D. Stranks^{1*}

¹Cavendish Laboratory, JJ Thomson Avenue, Cambridge CB3 0HE, United Kingdom

²Department of Chemical Engineering, Delft University of Technology, van der Maasweg 9, 2629 HZ Delft, The Netherlands.

³Clarendon Laboratory, Department of Physics, University of Oxford, Parks Road, Oxford OX1 3PU, United Kingdom

⁴Institute of Physics, Faculty of Physics, Astronomy and Informatics, Nicolaus Copernicus University, 5th Grudziądzka St., 87-100 Toruń, Poland.

PL spectrum fits in PL maps

The raw PL spectra are first denoised by subtracting the average of the first and last three points of all pixel in a map. A double pseudo-Voigt profile, corresponding to the linear sum of two pseudo-Voigt profiles which follow the formula presented by Thompson et al.,^[1] is then fit to every spectrum of the map. Each profile having its own amplitude, mean, Gaussian- and Lorentzian-width. The mean wavelength of the two fit pseudo-Voigt profiles are then compared for each pixel, with the lower mean wavelength and corresponding amplitude used for the WG peak, the higher mean wavelength and corresponding amplitude used for the LG peak. Hence, the amplitudes presented correspond to the pseudo-Voigt amplitudes, and the wavelengths to the mean of the profiles.

Fits to the time-resolved spectral data

The panels showing maximum intensity of PL peaks as a function of charge excitation density in Figure 3 were extracted from fits to the spectra with double Gaussian functions. The raw data, which were taken in different gains, were first corrected using a gain calibration file

for the CCD camera. A double Gaussian profile, which is the sum of two Gaussian functions with the formula of equation 1 was then fitted to each spectra, and the amplitude of the WG and LG peaks were extracted from the fits.

$$y = y_0 + A \exp\left(-\frac{(x-c)^2}{w^2}\right) + B \exp\left(-\frac{(x-s)^2}{v^2}\right) \quad (1)$$

The PL decays in Figure S14 were also extracted from fits to the time-evolving spectra with the same double Gaussian function.

Excitation density calculations

Excitation density of n_0 (cm^{-3}) can be expressed as:

$$n_0 = \frac{P(FA)}{A d h v (PRR)} \quad (2)$$

Where P is power (W), FA is fractional absorption, A is the beam spot size (cm^2), d is the thickness of the perovskite film (cm), h is Plank's constant (J.s), v is frequency of the laser light (Hz), and PRR is pulse repetition rate (kHz).

Meaning of Phase in PDS:

The obtained photothermal signal has a compound called phase. The phase data indicates that there is a time delay between the excitation of the sample and subsequent deflection of the beam, which is dependent on the heat diffusion of the sample. The amplitudes of the periodic temperature at the sample-fluid boundary is expressed as:^[2]

$$\theta = |\theta_0| \exp(i\gamma)$$

where $|\theta_0|$ is the amplitude of the sample surface temperature, and γ is the phase of the temperature variation with respect to the modulated heating beam.

If the material is uniform through the film, the phase does not change for different pump excitation wavelengths. In contrast, the phase of the photothermal deflection signal changes when the thermal properties of the sample varies through the depth of the sample and this may

be due to various reasons – change in material through the depth, change in optical density of the sample, etc.^[3] When a strong increase in the phase is observed, it is normally considered as surface absorption (if sample is both optically and thermally thin). This means that domains of absorption are more prevalent on the surface of the film than the bulk.

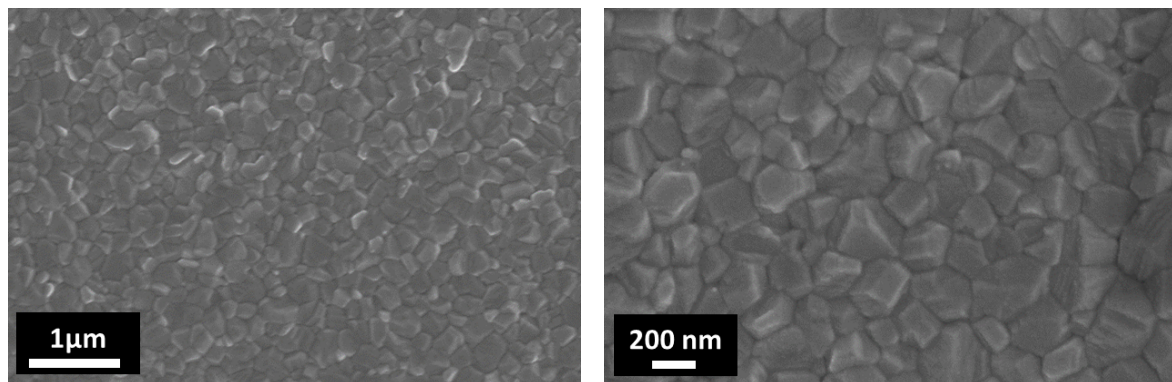


Figure S1. Top view SEM images of $(\text{Cs}_{0.06}\text{MA}_{0.15}\text{FA}_{0.79})\text{Pb}(\text{Br}_{0.4}\text{I}_{0.6})_3$ perovskite film formed on glass substrates with different magnifications.

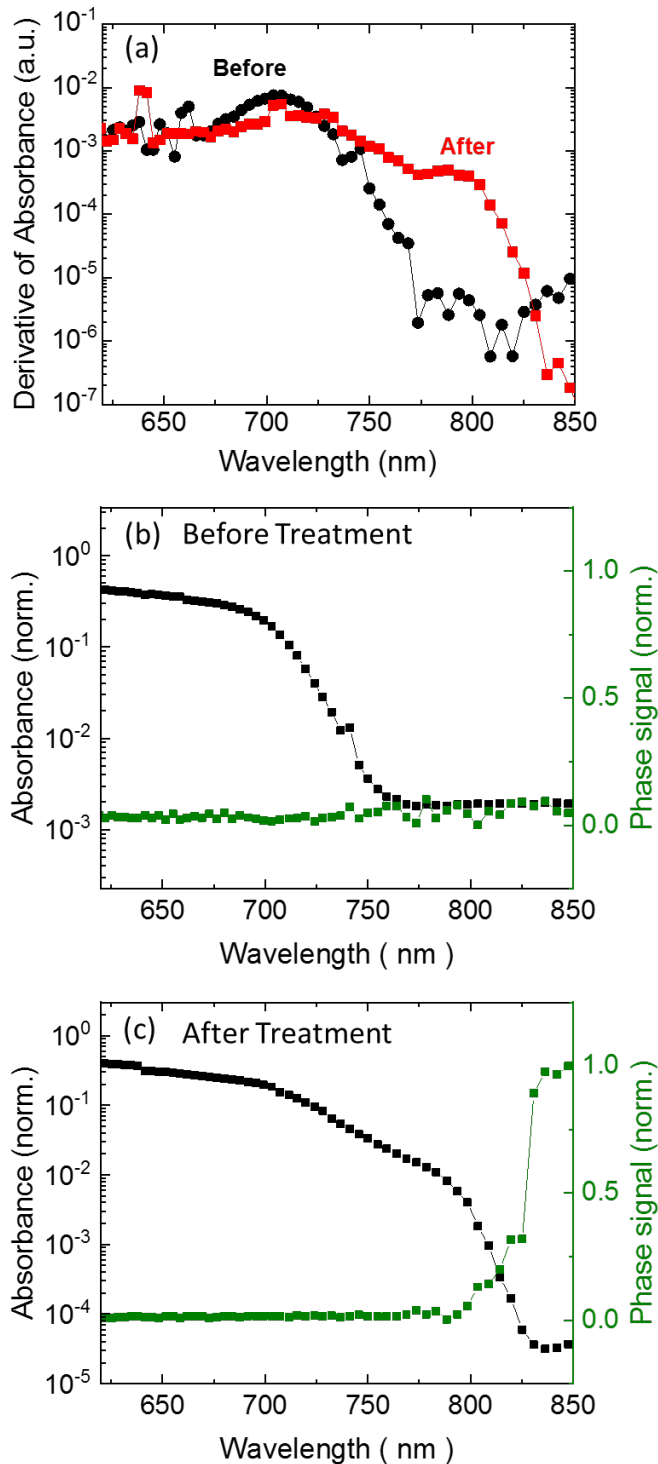


Figure S2. (a) The first derivative of Absorbance for PDS spectra shown in Figure 1a for the perovskite film before (black circles) and after (red squares) the light treatment. We used the derivative method to obtain the absorption edge of the higher- and lower-energy bandgap components. In this method, we take the derivative of the spectra and the position of the maximum intensity peak shows the absorption edge energy. Variation of PDS signal phase with wavelength for the perovskite film (b) before and (c) after the treatment. Note that the phase numbers are arbitrary and we have set the phase baseline to zero.

As we can see from Figure S2b and S2c, the phase is almost constant with wavelength for the film before treatment, but it undergoes a clear rise in the wavelengths from ~ 790 nm to ~ 840

nm after the treatment. Knowing that the samples are optically and thermally transparent before and after light treatment, the data suggests that the species absorbing in this range of wavelength could be more on the surface of the film than in the bulk.^[3] As LG regions have absorption in this range, we interpret this as there being a greater population of LG regions on the surface as compared to a change in the thermal properties of the bulk sample.

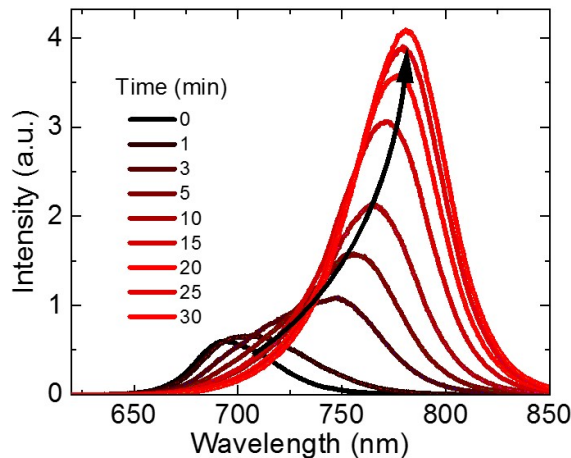


Figure S3. PL spectra of a perovskite film sandwiched between LED contact layers (zinc oxide nanoparticles doped with aluminum oxide as the electron injecting layer, and poly[(9,9-diptylfluorenyl-2,7-diyl)-co-(4,4-(N-(4-sec-butylphenyl)) diphenylamine)] (TFB) as the hole injecting layer) over time in ambient conditions under continuous laser illumination (532 nm laser, $\sim 60 \text{ mW/cm}^2$) producing the equivalent number of excitations to 1-sun intensity.

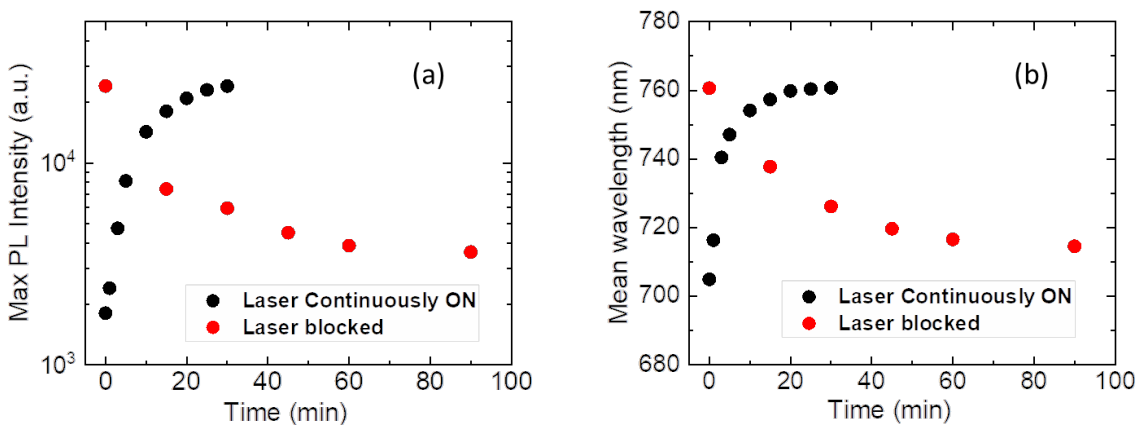


Figure S4. Growth and reversibility of (a) maximum PL intensity and (b) mean wavelength of perovskite film. The perovskite film was under continuous 532-nm laser illumination with intensity of 60 mW/cm^2 for 30 minutes to measure the growth of maximum PL intensity and mean wavelength, and was then put in dark (i.e. with the laser block) to measure the reversibility of the effects.

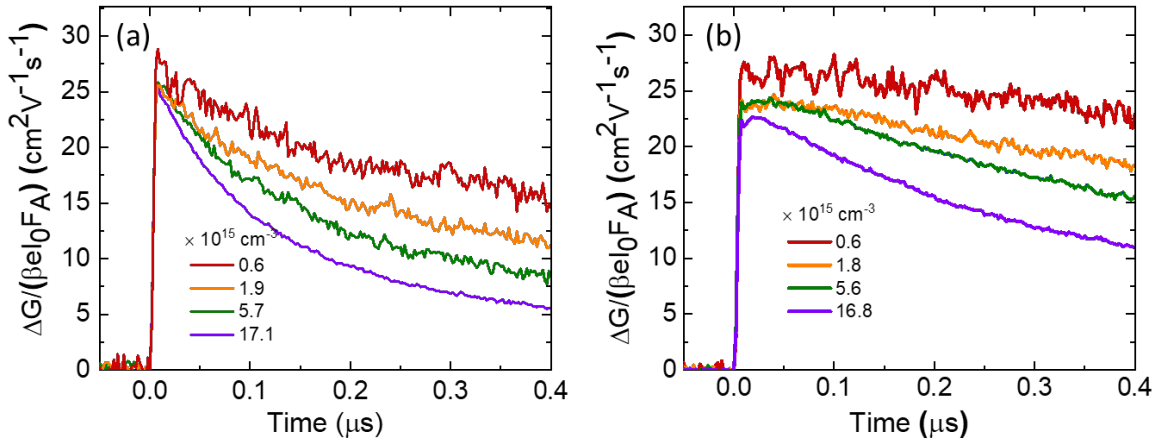


Figure S5. TRMC measurements performed on perovskite film, with excitation wavelength of 500 nm and different excitation fluences, before (a) and after (b) light treatment for 30 minutes under white light 1-sun-equivalent illumination. We observe a small rise component in ΔG during the initial time in the TRMC decay kinetics after light treatment in panel b; we propose that this initial rise behavior arises in part due to transfer of excitations from surface PbI_2 (on which charges are less mobile) to the LG perovskite regions.

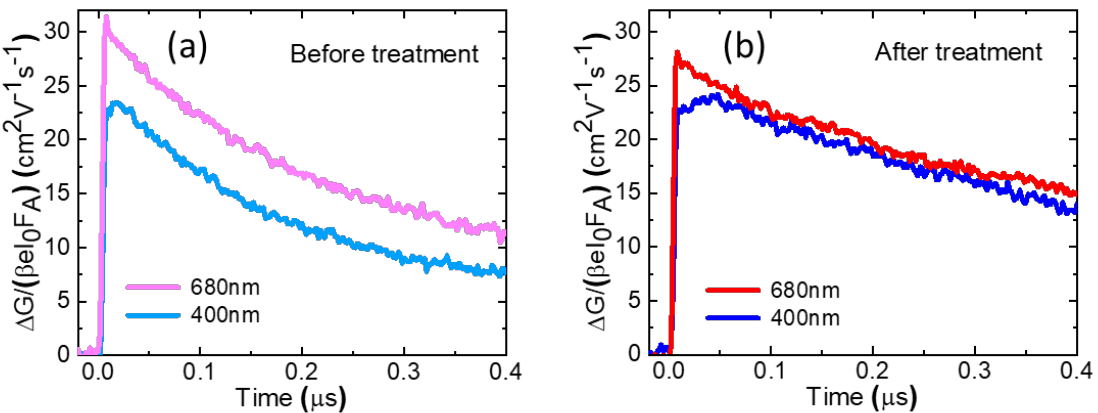


Figure S6. TRMC kinetics of the film for (a) before the treatment probed with excitations of 680 nm (Excitation fluence of $5.4 \times 10^{15} \text{ cm}^{-3}$), and 400 nm ($9.0 \times 10^{15} \text{ cm}^{-3}$), and (b) after the treatment probed with excitations of 680 nm ($5.3 \times 10^{15} \text{ cm}^{-3}$) and 400 nm ($8.0 \times 10^{15} \text{ cm}^{-3}$). From this figure, we observe that the rise component is more for 400 nm excitation, while the rise disappears when exciting at 680 nm. We suggest that this wavelength-dependent initial rise behavior is due to the transfer of charges from PbI_2 to the LG regions. PbI_2 with a bulk band gap of 2.36 eV^[4] can only absorb excitation wavelengths below 520 nm. When we excite the treated sample with excitations below this wavelength, some of the excited species initially reside on PbI_2 , which has low mobility of $\leq 8 \text{ cm}^2\text{V}^{-1}\text{s}^{-1}$ ^[5] and over time the charges transfer onto LG perovskite sites on which the mobilities are greater.^[6,7]

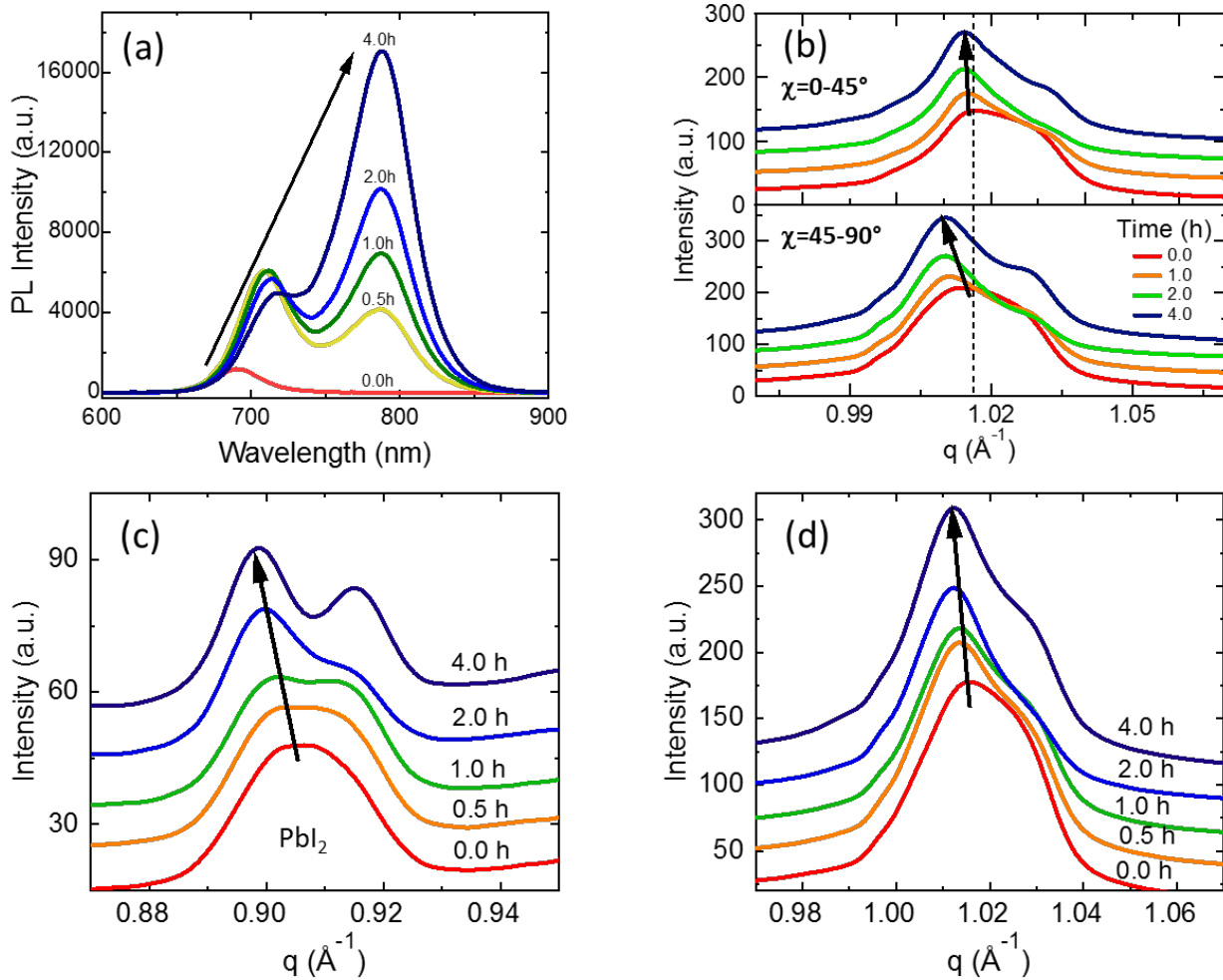


Figure S7. (a) PL spectra of $(\text{Cs}_{0.06}\text{MA}_{0.15}\text{FA}_{0.79})\text{Pb}(\text{Br}_{0.4}\text{I}_{0.6})_3$ film over time under laser illumination (532-nm laser, 0.3 suns) acquired simultaneously with the GIWAXS measurements in ambient atmosphere. (b) Out of plane ($0^\circ < \chi < 45^\circ$) and in-plane ($45^\circ < \chi < 90^\circ$) azimuthally integrated line profiles taken from GIWAXS profiles corresponding to the perovskite ($q \sim 1 \text{\AA}^{-1}$) peak for various time points under illumination (c) and (d) Integrated line profiles taken from GIWAXS profile corresponding to the PbI_2 ($q \sim 0.9 \text{\AA}^{-1}$) and perovskite ($q \sim 1 \text{\AA}^{-1}$) peaks at various time points under illumination.

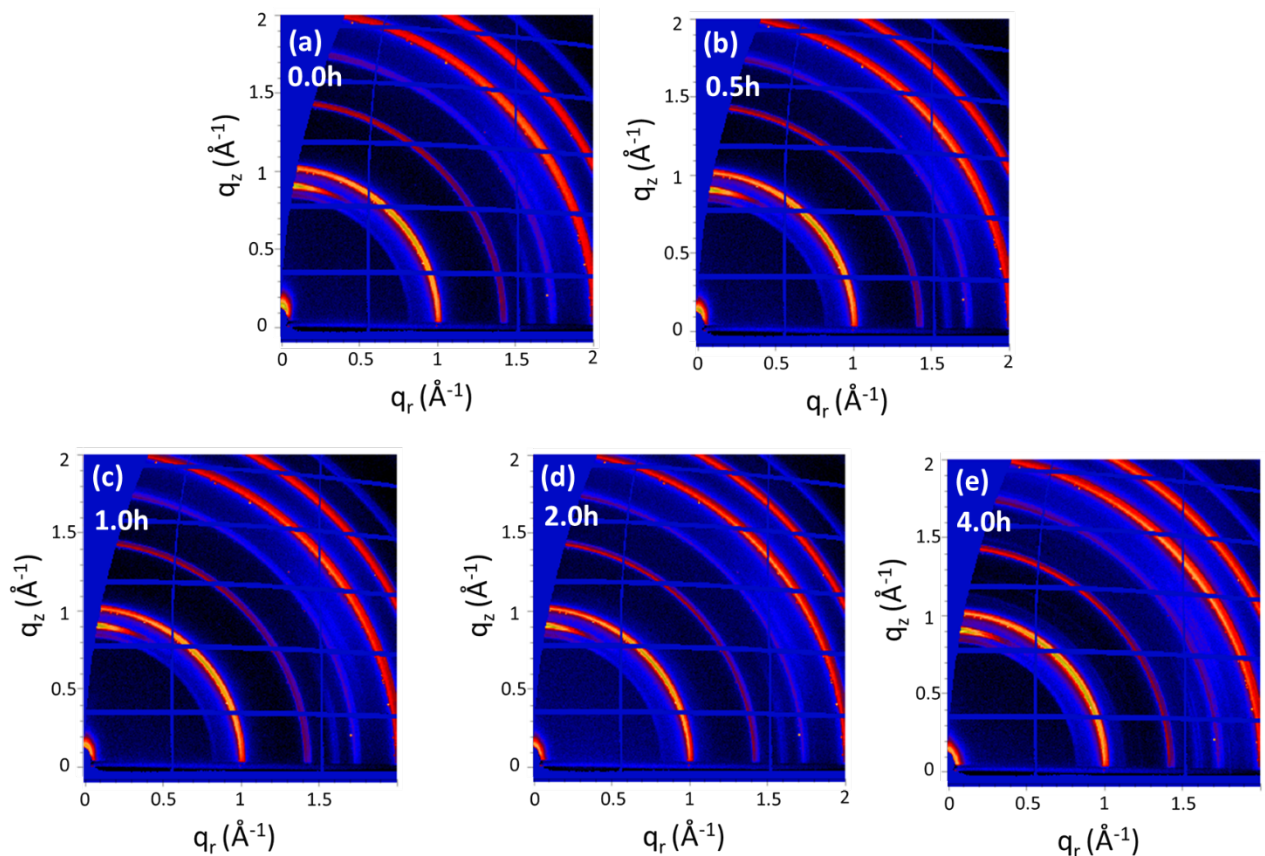


Figure S8. (a)-(e) Diffraction patterns collected at low angle using GIWAXS for perovskite film under the same laser illumination at various time points.

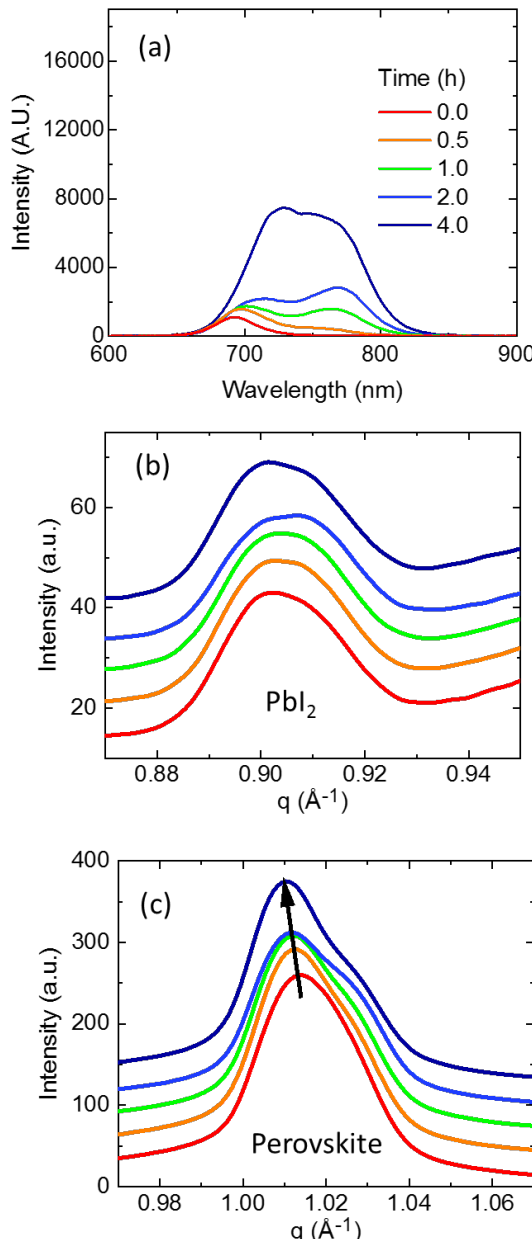


Figure S9. (a) PL spectra of $(\text{Cs}_{0.06}\text{MA}_{0.15}\text{FA}_{0.79})\text{Pb}(\text{Br}_{0.4}\text{I}_{0.6})_3$ film over time under laser illumination (532-nm laser, 0.3 suns) acquired simultaneously with the GIWAXS measurements in inert dry helium atmosphere (<5 % relative humidity). (b) and (c) Integrated line profiles taken from GIWAXS profile corresponding to the PbI_2 ($q \sim 0.9 \text{\AA}^{-1}$) and perovskite ($q \sim 1 \text{\AA}^{-1}$) peaks at various time points under illumination with a 532-nm laser at an intensity equivalent to 0.3 suns in Dry Helium atmosphere.

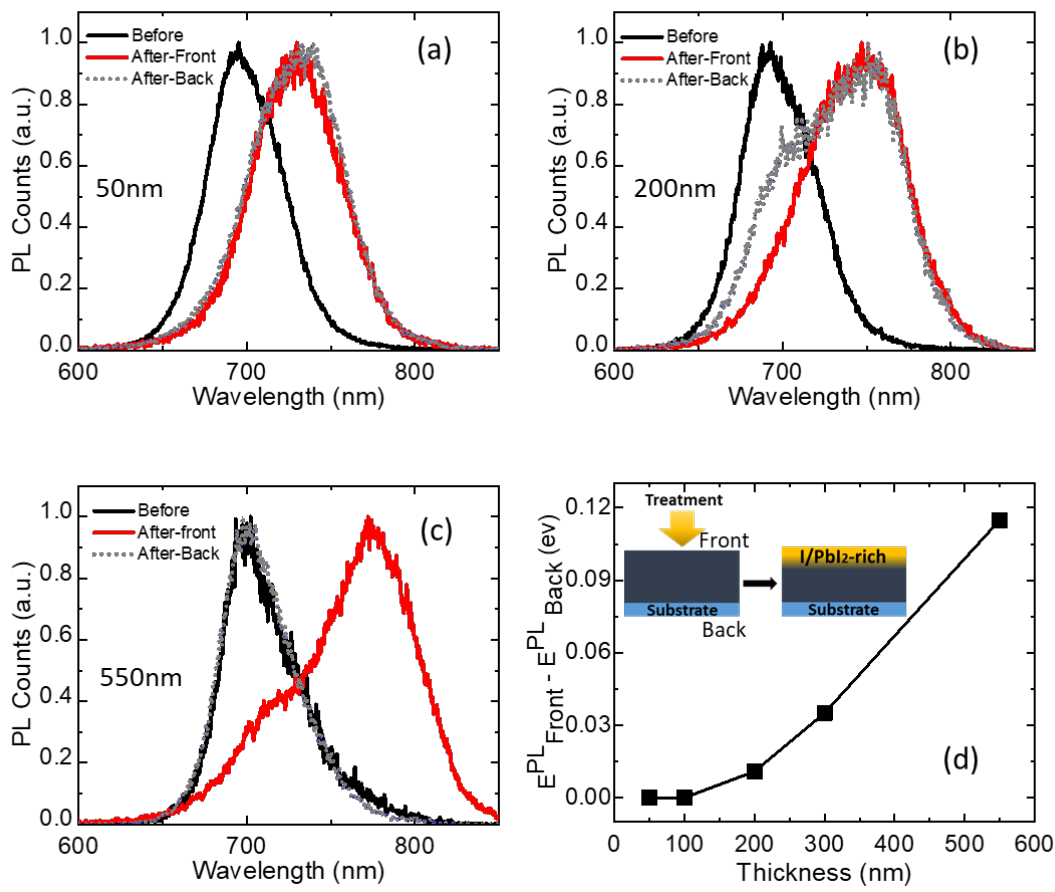


Figure S10. PL spectra of $(\text{Cs}_{0.06}\text{MA}_{0.15}\text{FA}_{0.79})\text{Pb}(\text{Br}_{0.4}\text{I}_{0.6})_3$ perovskite films with different thicknesses of (a) 50 nm, (b) 200 nm, and (c) 550 nm before and after light-treatment, probed from the front and back side of the film. We light-treated the films for 30 minutes with a white light LED source ($\sim 100 \text{ mW/cm}^2$). The PL was probed using a CW 405-nm laser ($\sim 10 \text{ mW/cm}^2$). (d) Difference between the mean PL energy (E^{PL}) measured from the front and back side of the sample with different thickness after light-treatment. Inset: Schematics that describe the measurement method and represent the proposed spatial distribution of the iodide-rich domains. We note that these PL measurements will include the process of carriers diffusing several hundreds of nanometres to the low bandgap surface sites even when exciting from the backside, and therefore they cannot alone be used to quantitatively assess the thickness of the surface layer.

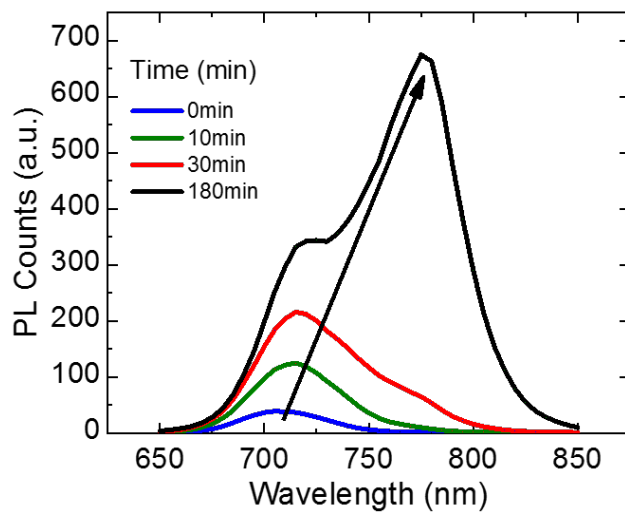


Figure S11. Spatially integrated PL spectra corresponding to the PL-mapped region in different light treatment times.

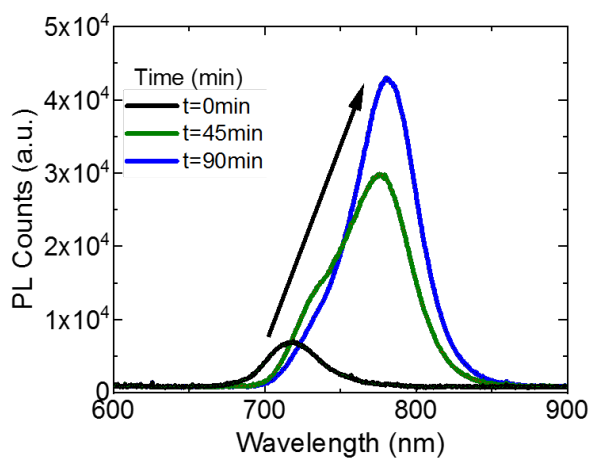


Figure S12. Steady state PL spectra of a $(\text{Cs}_{0.06}\text{MA}_{0.15}\text{FA}_{0.79})\text{Pb}(\text{Br}_{0.4}\text{I}_{0.6})_3$ perovskite film over time under laser illumination (532-nm laser, $\sim 60 \text{ mW/cm}^2$) collected via an optical fiber coupled to a spectrometer for the film before the treatment, after 45 min of treatment (partially treated), and after 90 min of treatment (fully treated). These measurements tracked the progress of the light treatment for the transient PL results shown in Figure 3.

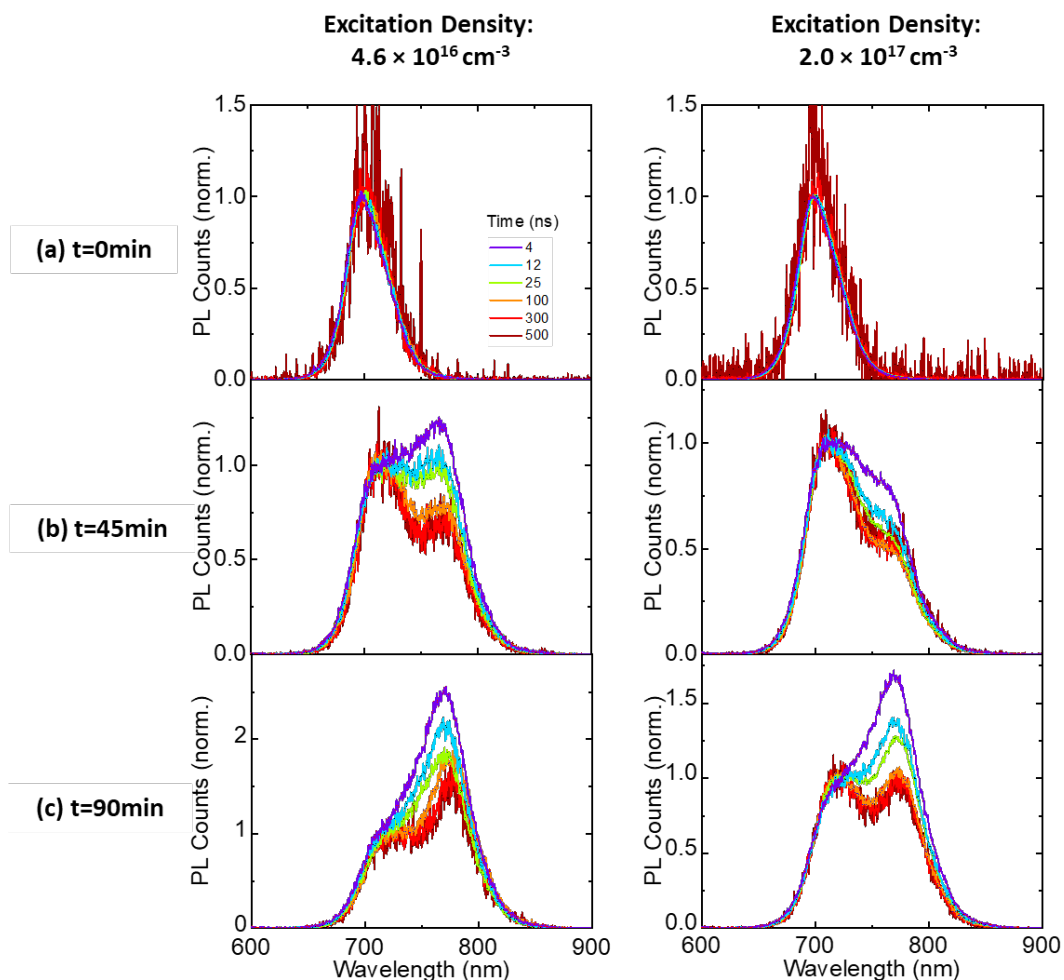


Figure S13. Transient photoluminescence spectra from perovskite films normalized at the WG peak probed following light soaking under laser illumination (CW 532-nm laser, $\sim 60 \text{ mW/cm}^2$) for (a) the film before the treatment, (b) after 45 min of treatment (partially treated), and (c) after 90 min of treatment (fully treated). The transient PL was probed using a pulsed 550-nm laser with two different fluences shown in the figure.

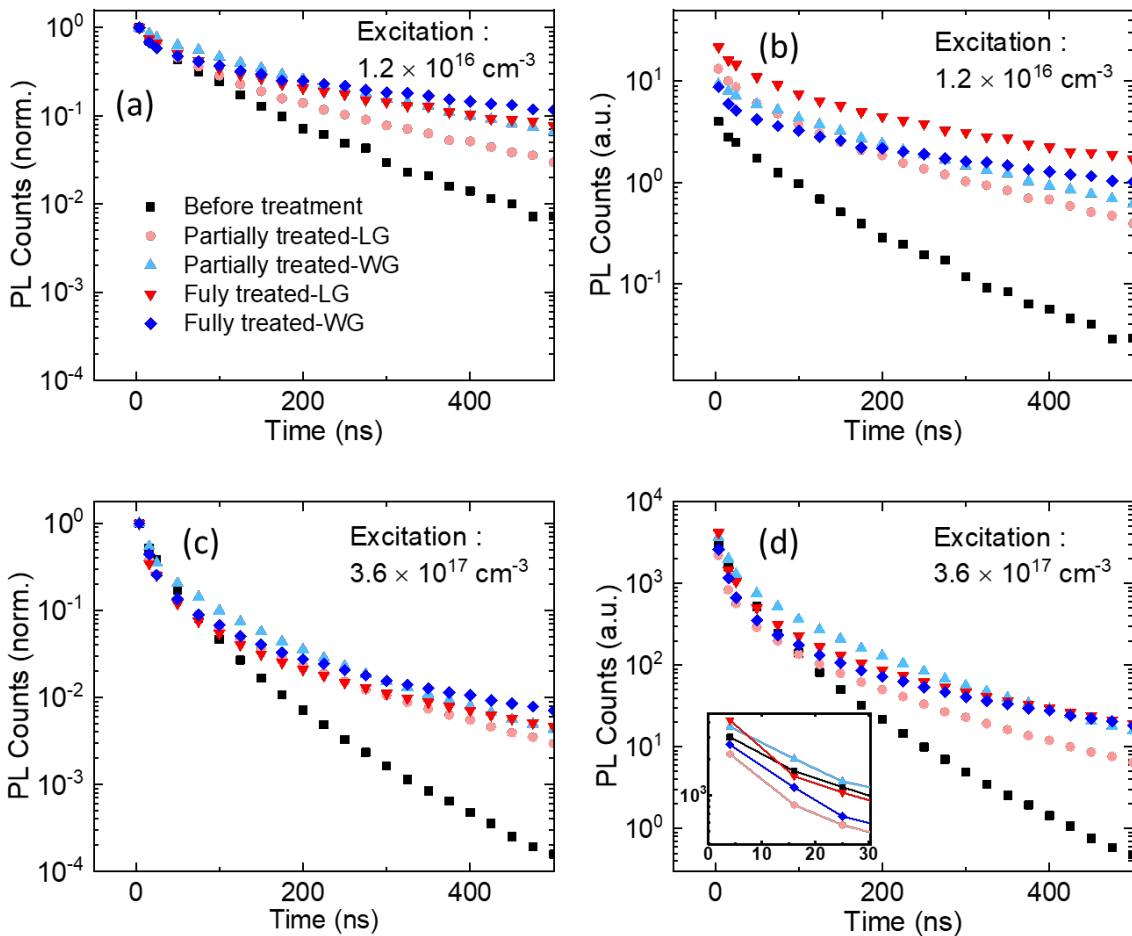


Figure S14. (a and b) PL kinetics for WG and LG peaks probed following light soaking under laser illumination (CW 532-nm laser, $\sim 60 \text{ mW/cm}^2$) in ambient conditions excited with a wavelength of 550 nm with intensity of $1.2 \times 10^{16} \text{ cm}^{-3}$ for the film before the treatment, after 45 min of treatment (partially treated), and after 90 min of treatment (fully treated). (c and d) The same measurement as above when the excitation density is $3.6 \times 10^{17} \text{ cm}^{-3}$. The inset in panel d shows a zoom in the initial time of decay.

Supporting References

- [1] P. Thompson, D. E. Cox, J. B. Hastings, *J. Appl. Crystallogr.* 1987, 20, 79.
- [2] Su, W.P., Schrieffer, J.R. & Heeger, A.J. *Phys. Rev. Lett.* 1979, 42, 1698.
- [3] J. P. Roger, D. Fournier, A. C. Boccara, F. Lepoutre, *Le J. Phys. Colloq.* 1989, 50, C5.
- [4] T. Supasai, N. Rujisamphan, K. Ullrich, A. Chemseddine, T. Dittrich, *Appl. Phys. Lett.* 2013, 103, 1.
- [5] F. Levy, C. Schwab, P. D. Bloch, J. W. Hodby, T. E. Jenkins, D. W. Stacey, G. Lang, F. Levy, C. Schwab, *J. Phys. C Solid State Phys.* 1978, 11, 4997.
- [6] E. M. Hutter, G. E. Eperon, S. D. Stranks, T. J. Savenije, *J. Phys. Chem. Lett.* 2015, 6, 3082.
- [7] R. Sheng, A. Ho-Baillie, S. Huang, S. Chen, X. Wen, X. Hao, M. A. Green, *J. Phys. Chem. C* 2015, 119, 3545.